Femtosecond time-resolved X-ray absorption spectroscopy of liquid using a hard X-ray free electron laser in a dual-beam dispersive detection method

Yuki Obara,[1] Tetsuo Katayama,[2] Yoshihiro Ogi,[3] Takayuki Suzuki,[1,4] Naoya Kurahashi,[5] Shutaro Karashima,[5] Yuhei Chiba,[1] Yusuke Isokawa,[1] Tadashi Togashi,[6] Yuichi Inubushi,[6] Makina Yabashi,[6] Toshinori Suzuki,[3,5] and Kazuhiko Misawa[1,4,*]

[1]Department of Applied Physics, Tokyo University of Agriculture and Technology, 2-24-16 Naka-cho, Koganei, Tokyo 184-8588, Japan
[2]Japan Synchrotron Radiation Research Institute, 1-1-1 Kouto, Sayo-cho, Sayo-gun, Hyogo 679-5198, Japan
[3]Molecular Reaction Dynamics Research Team, RIKEN Center for Advanced Photonics, 2-1 Hirosawa, Wako 351-0198, Japan
[4]Interdisciplinary Research Unit in Photon-nano Science, Tokyo University of Agriculture and Technology, 2-24-16 Naka-cho, Koganei, Tokyo 184-8588, Japan
[5]Department of Chemistry, Graduate School of Science, Kyoto University, Kitashirakawa-Oiwakecho, Sakyo-ku, Kyoto 606-8502, Japan
[6]RIKEN SPring-8 Center, 1-1-1 Kouto, Sayo-cho, Sayo-gun, Hyogo 679-5148, Japan
[*]kmisawa@cc.tuat.ac.jp

Abstract: We present femtosecond time-resolved X-ray absorption spectroscopy of aqueous solution using a hard x-ray free electron laser (SACLA) and a synchronized Ti:sapphire laser. The instrumental response time is 200 fs, and the repetition rate of measurement is 10 Hz. A cylindrical liquid beam 100 μm in diameter of aqueous ammonium iron(III) oxalate solution is photoexcited at 400 nm, and the transient X-ray absorption spectra are measured in the K-edge region of iron, 7.10 – 7.26 keV, using a dual X-ray beam dispersive detection method. Each of the dual beams has the pulse energy of 1.4 μJ, and pump-induced absorbance change on the order of 10^{-3} is successfully detected. The photoexcited iron complex exhibits a red shifted iron K-edge with the appearance time constant of 260 fs. The X-ray absorption difference spectra, with and without the pump pulses, are independent of time delay after 1.5 ps up to 100 ps, indicating that the photoexcited species is long-lived.

OCIS codes: (140.2600) Free-electron lasers (FELs); (320.7120) Ultrafast phenomena; (320.7150) Ultrafast spectroscopy.

References and links

1. T. J. Penfold, C. J. Milne, and M. Chergui, "Recent advances in ultrafast X-ray absorption spectroscopy of solutions," in *Advances in Chemical Physics*, S. A. Rice and A. R. Dinner, eds. (John Wiley, 2013), vol. 153.
2. L. X. Chen, "Probing transient molecular structures in photochemical processes using laser-initiated time-resolved X-ray absorption spectroscopy," Annu. Rev. Phys. Chem. **56**(1), 221–254 (2005).
3. L. X. Chen, W. J. H. Jäger, G. Jennings, D. J. Gosztola, A. Munkholm, and J. P. Hessler, "Capturing a photoexcited molecular structure through time-domain X-ray absorption fine structure," Science **292**(5515), 262–264 (2001).
4. J. J. Rehr and R. C. Albers, "Theoretical approaches to x-ray absorption fine structure," Rev. Mod. Phys. **72**(3), 621–654 (2000).
5. P. A. Lee, P. H. Citrin, P. Eisenberger, and B. M. Kincaid, "Extended X-ray absorption fine structure—its strengths and limitations as a structural tool," Rev. Mod. Phys. **53**(4), 769–806 (1981).
6. S. Nozawa, T. Sato, M. Chollet, K. Ichiyanagi, A. Tomita, H. Fujii, S. Adachi, and S. Y. Koshihara, "Direct Probing of spin state dynamics coupled with electronic and structural modifications by picosecond time-resolved XAFS," J. Am. Chem. Soc. **132**(1), 61–63 (2010).

#200512 - $15.00 USD Received 1 Nov 2013; revised 23 Dec 2013; accepted 23 Dec 2013; published 10 Jan 2014

7. R. W. Schoenlein, S. Chattopadhyay, H. H. W. Chong, T. E. Glover, P. A. Heimann, C. V. Shank, A. A. Zholents, and M. S. Zolotorev, "Generation of femtosecond pulses of synchrotron radiation," Science **287**(5461), 2237–2240 (2000).
8. S. Khan, K. Holldack, T. Kachel, R. Mitzner, and T. Quast, "Femtosecond undulator radiation from sliced electron bunches," Phys. Rev. Lett. **97**(7), 074801 (2006).
9. P. Beaud, S. L. Johnson, A. Streun, R. Abela, D. Abramsohn, D. Grolimund, F. Krasniqi, T. Schmidt, V. Schlott, and G. Ingold, "Spatiotemporal stability of a femtosecond hard-X-ray undulator source studied by control of coherent optical phonons," Phys. Rev. Lett. **99**(17), 174801 (2007).
10. Ch. Bressler, C. Milne, V.-T. Pham, A. Elnahhas, R. M. van der Veen, W. Gawelda, S. Johnson, P. Beaud, D. Grolimund, M. Kaiser, C. N. Borca, G. Ingold, R. Abela, and M. Chergui, "Femtosecond XANES study of the light-induced spin crossover dynamics in an iron(II) complex," Science **323**(5913), 489–492 (2009).
11. V.-T. Pham, T. J. Penfold, R. M. van der Veen, F. A. Lima, A. El Nahhas, S. L. Johnson, P. Beaud, R. Abela, C. Bressler, I. Tavernelli, C. J. Milne, and M. Chergui, "Probing the transition from hydrophilic to hydrophobic solvation with atomic scale resolution," J. Am. Chem. Soc. **133**(32), 12740–12748 (2011).
12. M. M. Murnane, H. C. Kapteyn, and R. W. Falcone, "High density plasmas produced by ultrafast laser pulses," Phys. Rev. Lett. **62**(2), 155–158 (1989).
13. F. Ráksi, K. R. Wilson, Z. Jiang, A. Ikhlef, C. Y. Côté, and J.-C. Kieffer, "Ultrafast X-ray absorption probing of a chemical reaction," J. Chem. Phys. **104**, 6066–6069 (1996).
14. J. Chen, H. Zhang, I. V. Tomov, M. Wolfsberg, X. Ding, and P. M. Rentzepis, "Transient structures and kinetics of the ferrioxalate redox reaction studied by time-resolved EXAFS, optical spectroscopy, and DFT," J. Phys. Chem. A **111**(38), 9326–9335 (2007).
15. W.-K. Chen, J. Chen, and P. M. Rentzepis, "Electron transfer mechanism in organometallic molecules studied by subpicosecond extended X-ray absorption fine structure spectroscopy," J. Phys. Chem. B **117**(16), 4332–4339 (2013).
16. P. Emma, R. Akre, J. Arthur, R. Bionta, C. Bostedt, J. Bozek, A. Brachmann, P. Bucksbaum, R. Coffee, F.-J. Decker, Y. Ding, D. Dowell, S. Edstrom, A. Fisher, J. Frisch, S. Gilevich, J. Hastings, G. Hays, Ph. Hering, Z. Huang, R. Iverson, H. Loos, M. Messerschmidt, A. Miahnahri, S. Moeller, H.-D. Nuhn, G. Pile, D. Ratner, J. Rzepiela, D. Schultz, T. Smith, P. Stefan, H. Tompkins, J. Turner, J. Welch, W. White, J. Wu, G. Yocky, and J. Galayda, "First lasing and operation of an Ångstrom-wavelength free-electron laser," Nat. Photonics **4**(9), 641–647 (2010).
17. T. Ishikawa, H. Aoyagi, T. Asaka, Y. Asano, N. Azumi, T. Bizen, H. Ego, K. Fukami, T. Fukui, Y. Furukawa, S. Goto, H. Hanaki, T. Hara, T. Hasegawa, T. Hatsui, A. Higashiya, T. Hirono, N. Hosoda, M. Ishii, T. Inagaki, Y. Inubushi, T. Itoga, Y. Joti, M. Kago, T. Kameshima, H. Kimura, Y. Kirihara, A. Kiyomichi, T. Kobayashi, C. Kondo, T. Kudo, H. Maesaka, X. M. Maréchal, T. Masuda, S. Matsubara, T. Matsumoto, T. Matsushita, S. Matsui, M. Nagasono, N. Nariyama, H. Ohashi, T. Ohata, T. Ohshima, S. Ono, Y. Otake, C. Saji, T. Sakurai, T. Sato, K. Sawada, T. Seike, K. Shirasawa, T. Sugimoto, S. Suzuki, S. Takahashi, H. Takebe, K. Takeshita, K. Tamasaku, H. Tanaka, R. Tanaka, T. Tanaka, T. Togashi, K. Togawa, A. Tokuhisa, H. Tomizawa, K. Tono, S. Wu, M. Yabashi, M. Yamaga, A. Yamashita, K. Yanagida, C. Zhang, T. Shintake, H. Kitamura, and N. Kumagai, "A compact X-ray free-electron laser emitting in the sub-Ångström region," Nat. Photonics **6**(8), 540–544 (2012).
18. Y. Inubushi, K. Tono, T. Togashi, T. Sato, T. Hatsui, T. Kameshima, K. Togawa, T. Hara, T. Tanaka, H. Tanaka, T. Ishikawa, and M. Yabashi, "Determination of the pulse duration of an X-ray free electron laser using highly resolved single-shot spectra," Phys. Rev. Lett. **109**(14), 144801 (2012).
19. H. T. Lemke, C. Bressler, L. X. Chen, D. M. Fritz, K. J. Gaffney, A. Galler, W. Gawelda, K. Haldrup, R. W. Hartsock, H. Ihee, J. Kim, K.-H. Kim, J.-H. Lee, M. M. Nielsen, A. B. Stickrath, W. Zhang, D. Zhu, and M. Cammarata, "Femtosecond X-ray absorption spectroscopy at a hard X-ray free electron laser: application to spin crossover dynamics," J. Phys. Chem. A **117**(4), 735–740 (2013).
20. R. Bonifacio, C. Pellegrini, and L. M. Narducci, "Collective instabilities and high-gain regime in a free electron laser," Opt. Commun. **50**(6), 373–378 (1984).
21. T. Katayama, Y. Inubushi, Y. Obara, T. Sato, T. Togashi, K. Tono, T. Hatsui, T. Kameshima, A. Bhattacharya, Y. Ogi, N. Kurahashi, K. Misawa, T. Suzuki, and M. Yabashi, "Femtosecond x-ray absorption spectroscopy with hard x-ray free electron laser," Appl. Phys. Lett. **103**(13), 131105 (2013).
22. C. A. Parker and C. G. Hatchard, "Photodecomposition of complex oxalates—some preliminary experiments by flash photolysis," J. Phys. Chem. **63**(1), 22–26 (1959).
23. B. A. DeGraff and G. D. Cooper, "Photochemistry of the ferrioxalate system," J. Phys. Chem. **75**(19), 2897–2902 (1971).
24. M. Yabashi, J. B. Hastings, M. S. Zolotorev, H. Mimura, H. Yumoto, S. Matsuyama, K. Yamauchi, and T. Ishikawa, "Single-shot spectrometry for X-ray free-electron lasers," Phys. Rev. Lett. **97**(8), 084802 (2006).
25. M. Saes, F. van Mourik, W. Gawelda, M. Kaiser, M. Chergui, C. Bressler, D. Grolimund, R. Abela, T. E. Glover, P. A. Heimann, R. W. Schoenlein, S. L. Johnson, A. M. Lindenberg, and R. W. Falcone, "A setup for ultrafast time-resolved X-ray absorption spectroscopy," Rev. Sci. Instrum. **75**(1), 24–30 (2004).
26. W. Gawelda, V.-T. Pham, M. Benfatto, Y. Zaushitsyn, M. Kaiser, D. Grolimund, S. L. Johnson, R. Abela, A. Hauser, C. Bressler, and M. Chergui, "Structural determination of a short-lived excited iron(II) complex by picosecond X-ray absorption spectroscopy," Phys. Rev. Lett. **98**(5), 057401 (2007).

#200512 - $15.00 USD Received 1 Nov 2013; revised 23 Dec 2013; accepted 23 Dec 2013; published 10 Jan 2014

1. Introduction

Time-resolved X-ray absorption spectroscopy (TRXAS) is useful for the studies of ultrafast electronic and structural dynamics of materials, as it enables element-selective observation of electronic states and the local geometrical structures in real time [1–3]. X-ray absorption near-edge spectroscopy measures the absorption spectrum near the ionization threshold, providing information on the local electronic state of the ionized atom [4]. Extended X-ray absorption fine-structure spectroscopy measures oscillatory structures in the absorption spectrum far above the ionization threshold, from which the distances and the number of atoms adjacent to the ionized atom can be determined [5].

TRXAS experiments are usually performed using synchrotron radiation; however, the electron bunch length in the storage ring limits the time resolution to tens of picoseconds [1,2,6]. The time-slicing technique, using the interaction of a femtosecond visible laser pulse with an electron bunch, improves the time resolution up to several hundred femtoseconds [7–9]. Although the slicing technique provides extremely low pulse energy, it has been successfully employed for TRXAS of liquids [10,11]. Femtosecond TRXAS experiments have also been performed with tabletop X-ray sources using laser-induced plasma on a metal wire [12–15]. The plasma emits X-ray radiation over large solid angles, so that only a small fraction can be utilized for TRXAS measurements; however, when the same driving laser is employed for generating both of the pump and probe pulses, accurate time delay is ensured.

Hard X-ray free electron lasers (XFELs), such as Linac Coherent Light Source (LCLS) [16] and SPring-8 Angstrom Compact Free Electron laser (SACLA) [17], are opening a new avenue for TRXAS. XFELs create intense X-ray pulses up to 10^{12} photons per pulse with a temporal duration down to 10 fs [18]. XAS is often performed by monitoring the total X-ray fluorescence as a function of the photon energy of monochromatized X-ray radiation. The fluorescence method has also been used in the first TRXAS experiment using LCLS [19]. However, since the repetition rates of XFELs are typically less than 100 Hz and considerable spectral fluctuations occur with SASE- (self amplification of spontaneous emission) XFELs [20], TRXAS using monochromatized X-ray radiation may not be most efficient. Recently, we proposed direct X-ray absorption spectroscopy using a dual-beam dispersive detection method as an alternative approach, which takes the advantage of broadband radiation, as large as 5×10^{-3} of $\Delta E / E$, from an unseeded FEL [21].

Here we present the first femtosecond TRXAS of $Fe(III)(C_2O_4)_3^{3-}$ in aqueous solution using the dual-beam dispersive detection method. We selected the iron oxalate complex [22,23], because its photo-induced dynamics is not well understood despite TRXAS studied by Rentzepis and associates using laser-plasma X-ray source [14]. The data acquisition, storage, and analysis are fully optimized and the pump-induced absorbance change on the order of 10^{-3} has been successfully detected.

2. Experimental

2.1 Experimental setup

Figure 1 shows our experimental setup for dual-beam dispersive detection. The XFEL output at a repetition rate of 20 Hz is divided using diffraction by a transmission grating. The + 1(upper) and −1(lower) order X-rays are used for simultaneous measurement of the signal and reference spectra, respectively. Each of these X-ray beams has 1.4 μJ of the incident pulse energy. Both beams are focused in a vertically long shape, 250 μm (vertical) by 25 μm (horizontal), using a single elliptical mirror, and only the + 1 order beam illuminate the sample and the −1 order beam does not. The X-ray fluence on the sample is as high as 29 mJ/cm^2. The zeroth-order undiffracted X-ray beam is blocked using a tungsten wire. The

#200512 - $15.00 USD Received 1 Nov 2013; revised 23 Dec 2013; accepted 23 Dec 2013; published 10 Jan 2014

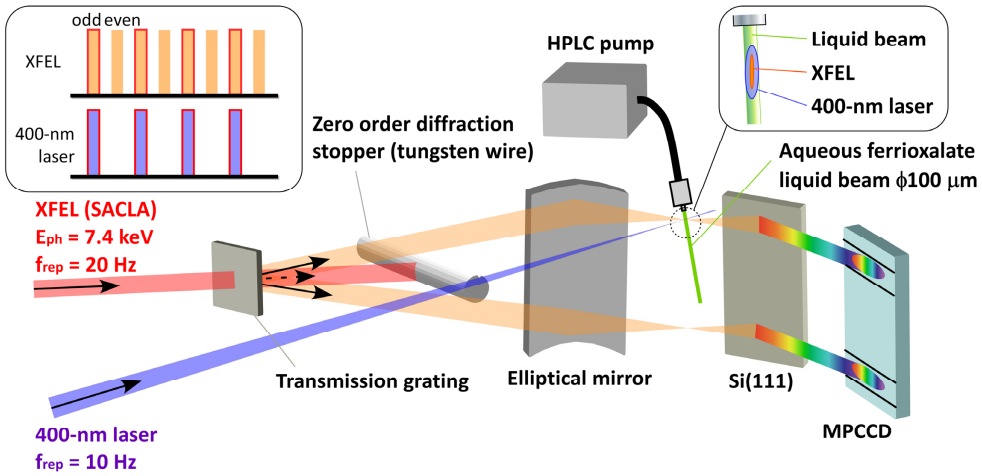

Fig. 1. Experimental setup for the dual-beam dispersive detection method. Spatial overlap of the sample liquid beam, pump laser and X-ray is depicted in the upper right inset. Temporal sequence of 400-nm pump and X-ray probe pulses is shown in the upper left inset. HPLC stands for high performance liquid chromatography.

0th and 1st orders cannot be measured simultaneously because the intensity of the 0th order is higher than that of ±1 orders by two orders of magnitude. Irradiation of the 0th order may cause a serious damage on the photodetector.

A dispersive spectrometer consists of an ultra-precisely figured elliptical mirror, a diffraction grating of a flat silicon (111) crystal, and a multi-port charge-coupled device (MPCCD) detector [24]. The signal and reference spectra are recorded simultaneously with the MPCCD for each XFEL shot to calculate the absorption spectra. The spectral range of the spectrometer is 67 eV, which is sufficiently wide to cover the entire XFEL bandwidth. The energy unit of one pixel in the dispersed direction is 0.35 eV, which we call "energy-bin" in the following, and the readout counts over 10 pixels in the direction perpendicular to the dispersed direction are summed up for one energy-bin. The spectral resolution of the system [21, 24] is determined by not only the pixel size but also the Darwin width of the Bragg reflection and it is estimated to be ca. 1 eV.

Femtosecond TRXAS is performed using a 400-nm second harmonic of a Ti:sapphire laser with a home-made double-pass power amplifier added to a commercial regenerative amplifier. The pump pulse has a temporal duration of 100 fs (FWHM). The repetition rate of the 400-nm laser is 10 Hz, so that the 400-nm pump pulses excite the sample for every other X-ray probe pulse from SACLA. The pulse energy is 1.1 mJ at the sample position, which corresponds to the photon number per pulse is on the order of 2.2×10^{15} . The fluctuation of the pulse energy is ± 2%. The focal area of the pump pulse is 400 μm (vertical) by 100 μm (horizontal), which is sufficiently large to cover the X-ray probe region fully. The fluence of 400-nm laser is 3.5 J/cm^2 on the sample. The 400-nm pump and X-ray probe beams are crossed at the sample with a small angle of less than 10 degrees.

The temporal jitter between the laser pulse and X-ray pulses were measured by cross-correlation technique using the fundamental frequency pulse from the Ti:sapphire laser. The jitter was determined to be 166 ± 8 fs from the FWHM of the Gaussian function by fitting the histogram of the timing fluctuation assuming a Gaussian distribution. Taking the 400-nm laser pulse width of 100 fs into account, the FWHM of the instrumental function is estimated to be 200 fs. On the other hand, the time origin between the 400-nm pulse and X-ray pulse drifted when measurements required a long time. Therefore, the time origin has been checked whenever necessary.

#200512 - $15.00 USD Received 1 Nov 2013; revised 23 Dec 2013; accepted 23 Dec 2013; published 10 Jan 2014

2.2 Data acquisition

The single-shot spectrum of XFEL has a spiky structure; however, the relative intensities of the spikes can be reduced by one order of magnitude by taking the difference spectrum of the signal and reference pulses, as shown in Fig. 2(a). Owing to the stochastic process in the SASE-XFEL, the spectrum of the X-ray pulse fluctuates on a shot-to-shot basis. However, when each of the spectra of even and odd numbered pulses is averaged over 500 pulses, the two spectra become almost identical, as shown in Fig. 2(b). The spectral difference of the two adjacent pulse spectra is 5 percent of the incident photon number per energy-bin in average.

In the present study pulse fluctuation is compensated by the simultaneous measurement of signal and reference spectra in the dual beam scheme. This dual beam scheme is combined with alternating excitation sequence. The bottom panel of Fig. 2(c) shows the difference in the odd and even numbered pulses between the signal and reference branch, whereas the top panel shows the difference between these two reference-compensated spectra. The fluctuation of the spectrum diminishes by two orders of magnitude after averaging over 500 shots.

We first measured XFEL spectra I, simultaneously for the signal and reference branches without the sample and calculated the following background spectrum, A_{bg},

$$A_{\mathrm{bg}} = -\log_{10}\left(I_{\mathrm{sig}}^{\text{w/o sample}} / I_{\mathrm{ref}}\right). \tag{1}$$

If the two spectra are identical, A_{bg} becomes entirely zero. In reality, the signal and reference branches do not provide the identical spectra, which gives rise to non-zero values in A_{bg}. Next, the absorption spectrum is obtained from the signal and reference X-ray spectra measured with a liquid beam as follows,

$$A_{\mathrm{sample}} = -\log_{10}\left(I_{\mathrm{sig}}^{\text{w sample}} / I_{\mathrm{ref}}\right). \tag{2}$$

If we average each of A_{bg} and A_{sample}, we obtain the sample absorption spectrum as follows,

$$A^{\mathrm{ave}} = A_{\mathrm{sample}}^{\mathrm{ave}} - A^{\mathrm{ave}}{}_{\mathrm{bg}}. \tag{3}$$

In pump-probe experiments, we have to record the sample absorption spectra with and without the pump pulse and obtain their difference spectrum. The spectra of the signal and reference branch are measured for every X-ray pulse while the pump pulse is irradiated for

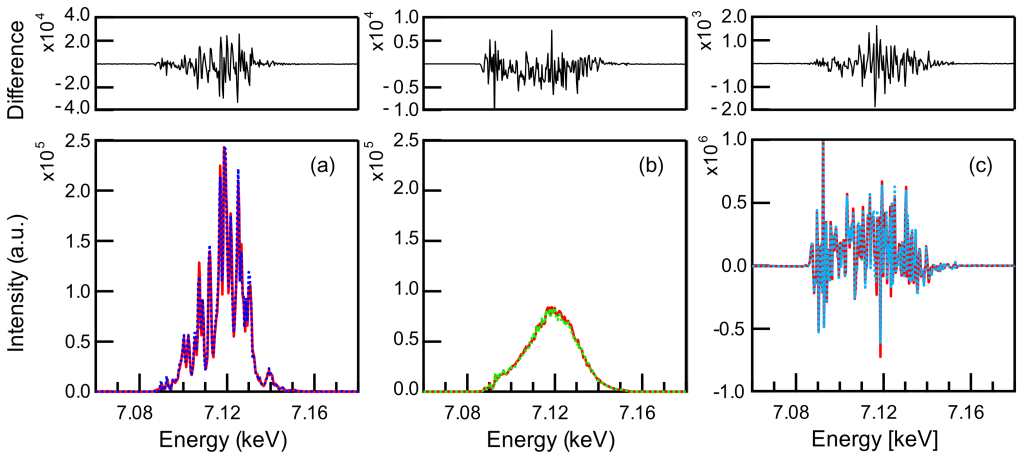

Fig. 2. Typical XFEL spectra (a) Typical dual-beam spectra of the signal (red solid line) and reference (blue dotted line) branches. (b) Averaged spectra of two adjacent even (red) and odd (green) numbered X-ray pulses over 500 shots. (c) Difference in the odd and even numbered pulses between the signal (red) and reference (blue) branch. Top panels show the difference between these two reference-compensated spectra.

#200512 - $15.00 USD Received 1 Nov 2013; revised 23 Dec 2013; accepted 23 Dec 2013; published 10 Jan 2014

every other X-ray pulse, as graphically represented in the upper left inset of Fig. 1. This alternating data acquisition scheme is similar to those employed with synchrotron radiation [25]. Then, the absorption spectra of the odd and even numbered X-ray pulses correspond to those with and without the pump pulses. Each of these spectra is averaged over at least 500 shots and their difference is taken as follows,

$$\Delta A^{\text{ave}} = A^{\text{ave}}_{\text{w pump}} - A^{\text{ave}}{}_{\text{w/o pump}} \tag{4}$$

2.3 Sample description

Aqueous solution of 0.5 M ammonium iron(III) oxalate trihydrate was discharged into air from a fused silica capillary with a 100-μm inner diameter and at a flow rate of 5 mL/min. The liquid beam is a cylindrical shape, and the flow speed is 10.6 m/sec. The sample concentration was selected to make the optical density for X-ray radiation reasonably high; the molar extinction coefficient ε at the K-edge of iron (7.1 keV) is 22.8 $cm^{-1}M^{-1}$ and the absorbance for 0.5 M aqueous solution is about 0.1. For observing the pump-probe signal, we need to photoexcite a large fraction of molecules in the observation region with the pump pulse. The number of iron complexes in the volume illuminated by X-ray is estimated as 1.5×10^{14}. Since the molar extinction coefficient at 400 nm is 160 $cm^{-1}M^{-1}$ [14], photon numbers more than 8.8×10^{13} is required for pumping a half of these complexes to the excited state. In terms of laser pulse energy this is 44 μJ/pulse. Since the pump laser spot size is 6.4 times larger, the pump pulse energy should be at least 280 μJ/pulse. Thus, we employed a rather intense pump pulse (1.1-mJ).

A fresh sample solution kept in a container covered with aluminum foil was used for measurements, and the discharged solution from the nozzle was disposed. We did not recirculate the sample solution for measurements to avoid buildup of the concentration of photodissociated products. The liquid flow rate and hydrodynamic stabilities were continuously monitored using a high-pressure chromatography pump and a CCD camera, respectively. Entire experiments were performed at room temperature and under atmospheric pressure.

3. Results

Figure 3(a) shows the difference X-ray absorption spectra of the $Fe(III)(C_2O_4)_3^{3-}$ complex around the K-edge of the Fe atom at several pump-probe time delays. Each difference spectrum is calculated from the absorption spectra with and without the pump pulses accumulated over 10000 shots and it takes 17 minutes to take one difference spectrum. A positive absorbance change indicates an increased absorption by 400-nm photoexcitation. The peak position appearing at 7.12 keV is lower than the K-edge of the steady-state spectrum of the molecule. The shape of the difference spectra does not vary with the time delay.

Figure 3(b) shows the temporal dependence of the absorbance change integrated over 7.120 ± 0.006 keV. Assuming the instrumental response time of 200 fs expected from timing jitter of the X-ray pulse and the duration of 400-nm pulse, the least squares fitting of the experimental data provides the rise time of 260 ± 50 fs as shown in solid line.

Figures 4(a) and 4(b) present the spectra of X-ray pulses and difference absorption spectra for wider energy regions, respectively. We employed five different central photon energies, as shown in different colors in Fig. 4(a), by changing the undulator setting to observe the energy region of 7.10 – 7.26 keV. The difference spectra merged from five spectra taken for different energy regions are shown in Fig. 4(b) at six time delays. The spectral profile is essentially the same even at a time delay of 100 ps.

#200512 - $15.00 USD Received 1 Nov 2013; revised 23 Dec 2013; accepted 23 Dec 2013; published 10 Jan 2014

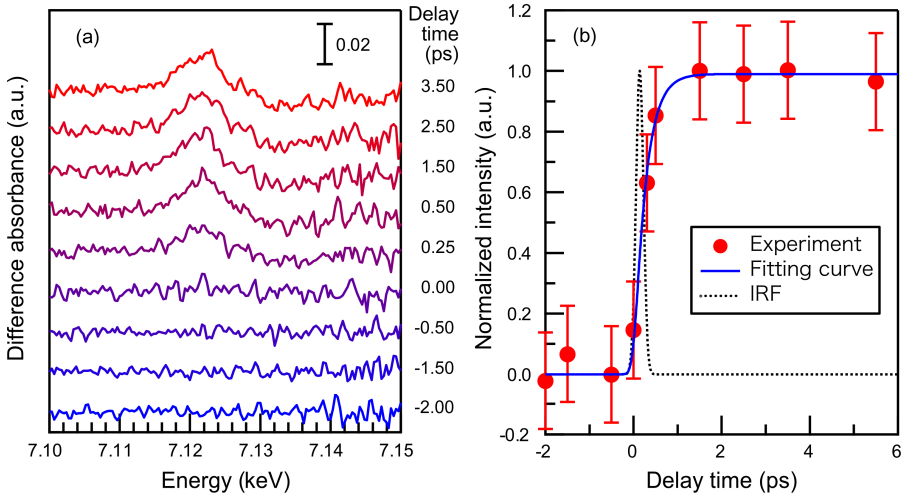

Fig. 3. Time-resolved difference absorption spectra and its transients. (a) Time-resolved difference X-ray absorption spectra of aqueous 0.5 M ammonium iron(III) oxalate trihydrate solution. (b) Temporal dependence of the absorbance change integrated over 7.120 ± 0.006 keV in the difference absorption spectra.

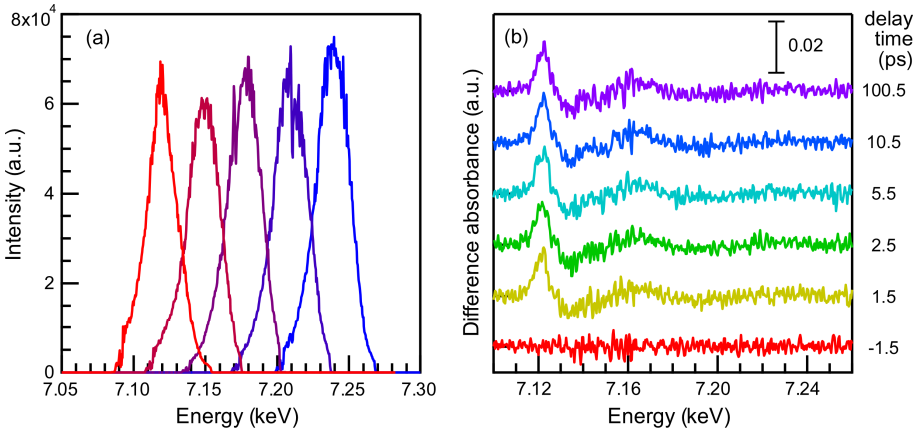

Fig. 4. Extended difference absorption spectra (a) Five different XFEL spectra employed to measure the transient absorption spectra for 7.10 – 7.26 keV. Each difference spectrum is calculated from the absorption spectra with and without the pump pulses accumulated over 10000 shots. (b) Time-resolved difference absorption spectra. Each spectrum is constructed from five spectra of different energy regions.

4. Discussion and conclusion

4.1 Estimation of detection limit

The largest absorbance change seen in Fig. 3 is 0.02, whereas the rms of the fluctuation in absorbance change is 0.002 in the present experiment. Let us compare these values with the minimal detection limit expected under the present experimental condition. The pulse energy of the probe X-ray at 7.12 keV is 1.4 μJ just after diffracted at the beam splitter, which corresponds to the photon number of 1.2×10^{9}. The effective photon number limited by the acceptance of the elliptical mirror is 7% of the incident pulse. The transmission of the sample is $10^{-0.1}$. The diffraction efficiency of the monochromator crystal is 4×10^{-3} determined by the ratio of Darwin width and the divergence of the X-ray beam as well as the polarization factor. The transmission loss of X-ray in air through its entire path is 60%. The reciprocal linear

#200512 - $15.00 USD Received 1 Nov 2013; revised 23 Dec 2013; accepted 23 Dec 2013; published 10 Jan 2014

dispersion of the monochromator crystal is 0.35 eV/pixel, hence X-ray pulses with the bandwidth of 30 eV is dispersed in one pixel by the factor of 0.35/60 in average. Taking all the above factors into consideration, the average photon number per pulse arriving at one channel on the MPCCD detector can be predicted as $1.2\times10^{9}\times0.07\times4\times10^{-3}\times10^{-0.1}\times(1-0.6)\times(0.35/60)=6.2\times10^{2}$.

The average number of photons actually arriving at the MPCCD can be estimated from the average readout count of MPCCD, which corresponds to $9\times10^{5}e^{-}$ per X-ray pulse for one energy-bin. Since MPCCD generates $2\times10^{3}e^{-}$ for each incoming X-ray photon at 7.12 keV and the quantum efficiency of conversion from a photon to an electron-hole pair is 0.6 at 7 keV, the photon number arriving at the detector for each energy-bin is

$$9\times10^{5}/\left(2\times10^{3}\right)/0.6=7.5\times10^{2}.$$

Thus, the predicted and observed photon numbers are in reasonable agreement.

The absorbance change of 0.02 corresponds to variation of the arriving photon numbers by 35 photons/pulse, so that the fluctuation of 0.002 is equivalent to 3.5 photons. Note that the system noise per energy bin (10 pixels of the MPCCD) is about 3.5×10^{3} electrons, corresponding to 1.75 photons. Thus, we speculate that the system noise of the detector is an important factor for the minimal detection limit under the present experimental condition, although more detailed analysis must be performed.

4.2 Retrieval of excited state spectrum

The difference absorption spectrum ΔA is defined as

$$\Delta A = f\left[A_{\mathrm{ex}} - A_{\mathrm{nonex}}\right], \tag{5}$$

where A_{ex} and A_{nonex} are the spectra of the excited and nonexcited molecular species, respectively, and f is the fractional population of the excited species. A_{ex} can be retrieved from the measured spectra with and without pump, $A^{\mathrm{ave}}_{\mathrm{w\ pump}}$ and $A^{\mathrm{ave}}{}_{\mathrm{w/o\ pump}}$, using the following relation,

$$A_{\mathrm{ex}} = A^{\mathrm{ave}}_{\mathrm{w/o\ pump}} + \frac{1}{f}\left[A^{\mathrm{ave}}_{\mathrm{w\ pump}} - A^{\mathrm{ave}}_{\mathrm{w/o\ pump}}\right] \tag{6}$$

if f is known [26]; f should be determined individually in most cases.

In the present experiment, we employed 1.1-mJ pump energy four times larger than the expected value necessary for exciting a half of the molecules. Assuming $f = 0.5$ we obtained the excited-state spectrum A_{ex} as shown in blue in Fig. 5(a). We compared the retrieved spectra for several parameters of fractional population around $f = 0.5$, and found that while the K-edge shift varies with f, other spectral features were rather insensitive to f.

Our result indicates that the transient species has a rather similar geometrical structure with the ground state complex and its lifetime is longer than 100 ps. It has been generally accepted that light-induced electron transfer reduces the Fe(III) complex to the Fe(II) complex [22]. One of the proposals for photodynamics of $Fe(III)(C_2O_4)_3^{3-}$ was intramolecular ligand-metal electron-transfer [23]. An alternative proposal was photodissociation while maintaining the oxidation number of + 3 [14]. In any case, the observed red-shift of the K-edge indicates that the electron density of the excited Fe(III) has increased compared to the ground state. With the limited experimental evidences from our study, the assignment of this transient species cannot be readily made. Further information such as transient infrared absorption spectra, the lifetime measurements and kinetic analysis, or even higher time resolution in TRXAS will be of assistance for elucidating its chemical nature.

#200512 - $15.00 USD Received 1 Nov 2013; revised 23 Dec 2013; accepted 23 Dec 2013; published 10 Jan 2014

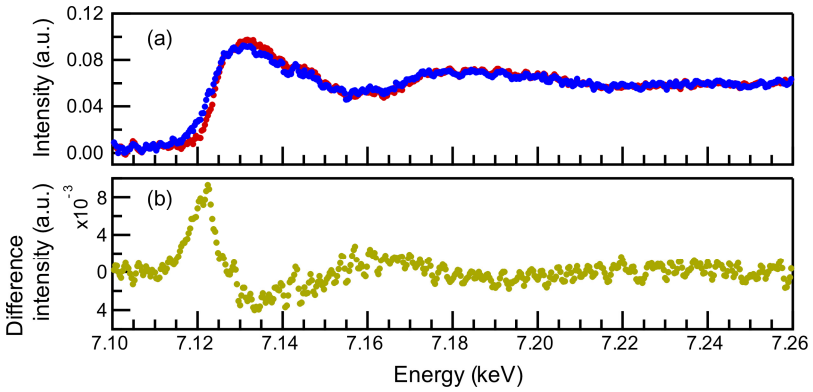

Fig. 5. (a) Estimated spectrum of the excited species assuming the excitation yield of 50% (red) and measured spectrum of unexcited molecules (blue); (b) measured difference spectrum at 1.5 ps

In conclusion, the first time-resolved X-ray absorption spectroscopy using SACLA was performed using a dual X-ray beam dispersive detection method for aqueous 0.5 M ammonium iron(III) oxalate trihydrate solution. Applications to other solid and liquid samples are readily possible. The method is expected to be even more useful in the soft X-ray region, where the X-ray absorption cross section is considerably larger than in the hard X-ray region.

Acknowledgments

We thank the operation and engineering staff of SACLA for their support in carrying out the experiment. The XFEL experiments were performed at the BL3 of SACLA with the approval of the Japan Synchrotron Radiation Research Institute (JASRI) (Proposal No. 2013A8059). This work was partially supported by the "X-ray Free Electron Laser Priority Strategy Program" of the Ministry of Education, Culture, Sports, Science and Technology, Japan (MEXT).